

Thin-film iron-catalyzed “beads on a string” carbon nanotubes

Johnathan Goodsell¹, Stephanie A. Getty², Jon Brame¹, and David D. Allred¹

NASA Brigham Young University

¹ *Department of Physics and Astronomy, N283 ESC, Brigham Young University, Provo, UT, 84602*

² *NASA Goddard Space Flight Center, Materials Engineering Branch, Code 541, Greenbelt, MD, 20771*

(Received: ; accepted)

We report on the iron-catalyzed, CVD growth of carbon nanotubes on a variety of substrates and their subsequent analysis. We discuss the use of “indirect evaporation” to prepare the required iron catalyst. The optimum temperature for growth of nanotubes mats was between 925 and 950 degrees C. These were shown by transmission electron microscopy to contain single-walled carbon nanotubes (SWCNTs). We examined the results of the deposition in scanning electron microscopy and saw what appeared to be bright spots randomly arrayed along the carbon nanotube fibers. We termed this pattern ‘beads on a string’. We present evidence that the bright features are not associated with the nanotubes directly but are iron/carbon clusters that happen to lie on the surface of the substrate near where the tubes fell during or after deposition. We have shown that the deposition procedure is fairly robust and growth results have been reproduced using Goddard Space Flight Center (GSFC)-deposited catalyst and CVD facilities at Brigham Young University (BYU). © 2007 Utah Academy.

1. INTRODUCTION

Because of their remarkable electronic and mechanical properties, carbon nanotubes, particularly single-walled carbon nanotubes (SWCNTs) have been the subject of intensive research efforts over the past decade. The bonding structure of carbon nanotubes is sp^2 , as in graphite. Rather than lay flat as a single sheet of graphite, however, it is as though a thin strip of graphene is rolled up to form a seamless tube.¹ The length to width ratio, or aspect ratio, for these tubes can be in the millions - extremely high for any material, and SWCNTs can be stronger per weight than steel.

An additional property, the focus of this investigation, is that as the tubes are stretched or strained their electrical resistance increases.¹⁻⁵ This large strain-induced response in electronic resistance, suggests their application in strain sensing devices.⁶⁻⁸ We have selected a network of SWCNTs to develop one such strain sensing device for magnetic field detection, where the ensemble properties of the nanotube network ensures adequate mechanical stability of the NEMS device and promotes inter-device uniformity in electromechanical response. Facing low density nanotube growth using solution-deposited iron nitrate as catalyst, we sought to achieve a denser growth of a network of SWCNTs by chemical vapor deposition (CVD).⁸⁻⁹ The literature suggested the use of thin film deposited iron catalyst to achieve higher nanotube density.⁸⁻¹¹ The most reliable method we found for depositing this ultrathin iron layer (<1 nm) was by facing the substrate *away from* the evaporation source. After growing the nanotubes, we viewed the

SWCNT network via scanning electron microscopy and discovered a particular pattern of bright spots along nanotubes, which has not been previously discussed. We refer to this pattern as “Beads on a String” (BoS). Investigations into the composition of the BoS pattern and how it arises are discussed below.

2. METHOD

A. Indirect Thin Film Iron Deposition

The SWCNTs were grown using an iron catalyst chemical vapor deposition (CVD) process. The substrate was single crystal silicon (100) with an approximate 500 nm-thick thermal oxide. Before this study, the catalyst had been prepared using a well-documented process of dipping the substrate in iron nitrate.⁷⁻⁸ This resulted in sparse growth of short tubes. The use of vacuum-deposited thin film iron was also documented in the literature⁹⁻¹¹ and led us to explore its use as a catalyst for dense SWCNT growth. The thickness generally used is, however, remarkably thin, usually less than one nanometer effective thickness and the effective thickness must be tightly controlled.

To produce such a very "light" deposition with thickness control to better than 0.1 nm by evaporation can be quite challenging. Usually one carefully places the substrate which is to receive the evaporated iron atoms a known distance above the resistively heated boat which holds the iron. The substrate faces the boat. Usually a moveable shutter and one or more water cooled thickness monitors are also required. The moveable shutter lies between the boat and the substrate but can be moved out of the way at the desired time in the deposition process to allow line-of-sight atoms from the source to reach the substrate, depositing the film. To control the thickness of the film a thickness monitor is also required, with sensitivity to 0.1nm, which can see the evaporation boat even with the shutter closed. One normally begins the process by bringing the substrate pressure to a base pressure in the low 10^{-6} Torr range. Next, by applying and increasing the voltage across the evaporation boat it is heated *with* the shutter closed. This allows one to reach a temperature where evaporation is beginning and to establish the rate without the surface of the sample seeing the direct flux of atoms which are streaming out of the source. When all is ready the shutter is move out of the way and iron atoms leaving the boat on a line of sight path reach the surface of the substrate, depositing the film.

This mode of evaporation is well suited for preparing thin films with an effective thickness of greater than 1 nm. There are several reasons why it is not well suited for films < 1nm. While one is establishing the deposition rate some atoms may be reaching the substrate by bouncing off residual gas molecules or the chamber walls. This results in an error of order 0.1-1nm in the thickness measurement recorded by the thickness monitor. Another reason is that quartz-crystal thickness monitors are usually temperature sensitive. When it is exposed to the heat coming off from the evaporation boat, its zero can drift negative by an nm or more, often indicating that the film is less thick than it actually is. This issue is exacerbated by the high melting temperature of iron. Many people water cool their monitors, but this adds cost and complexity to the system.

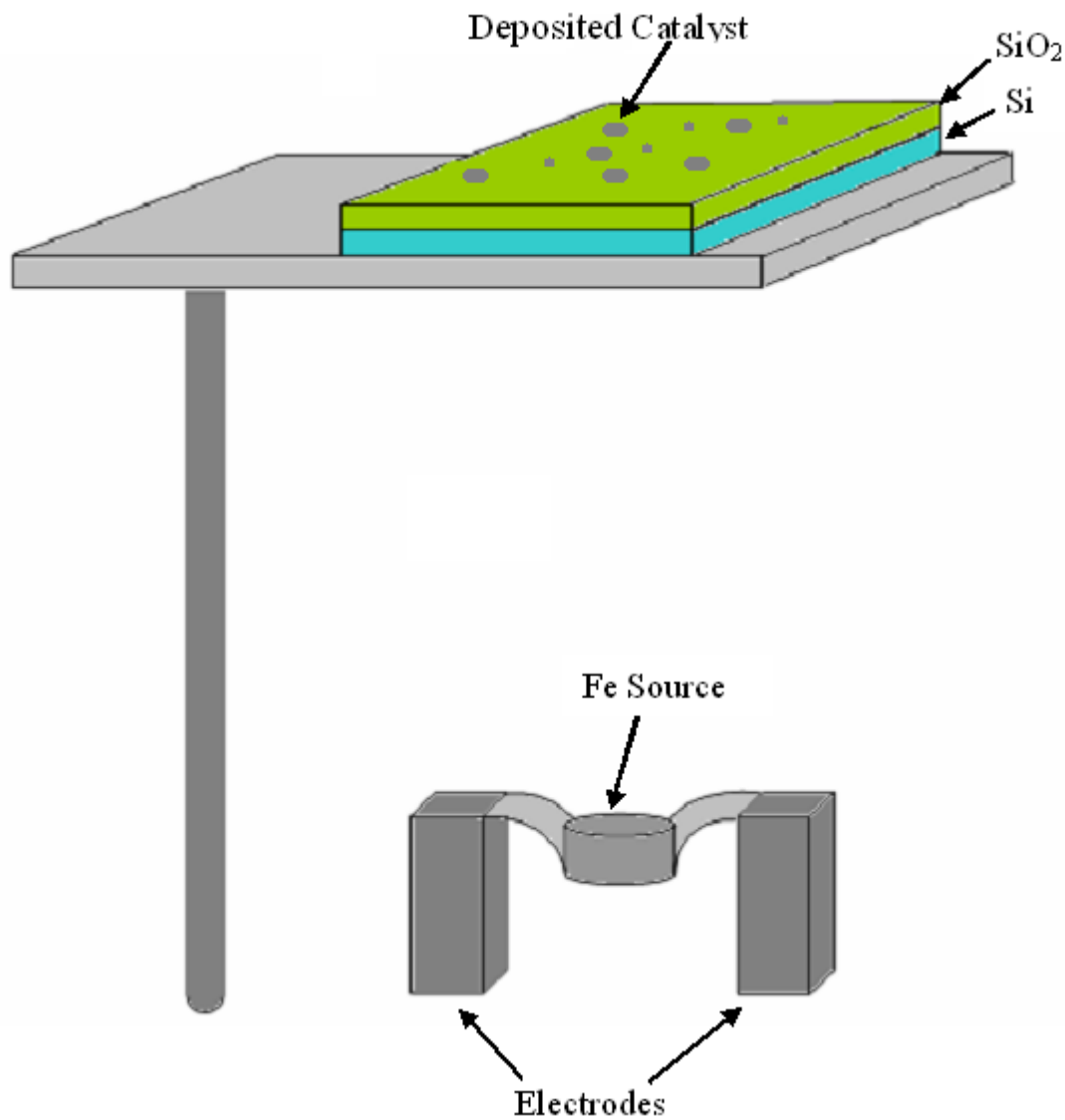


Figure 1: Iron catalyst was deposited using an indirect evaporation method, in which the substrate faces away from and out of the line-of-sight of the source (not to scale).

Early in this work at GSFC a much simpler method, indirect evaporation, was discovered. This procedure is shown in Figure 1. In contrast to traditional, direct thin-film evaporation described above, the substrate was oriented to face *away* from the iron source; the direct path from the source to the substrate was blocked by the sample holder, and no shutter was used. Iron was then evaporated at a rate of 0.05nm/s to a thickness of 10nm according to the thickness monitor, which was not water cooled. Iron deposition onto the substrate is accomplished through collisions with residual gas molecules and nearby surfaces within the chamber. It should be noted that this thickness measured by the thickness monitor is necessarily much greater than the actual thickness of the iron layer had on the side facing a way from the deposition source. The deposition was at approximately 10^{-6} Torr in the high vacuum chamber.

B. CVD Growth and Optimization of CNT

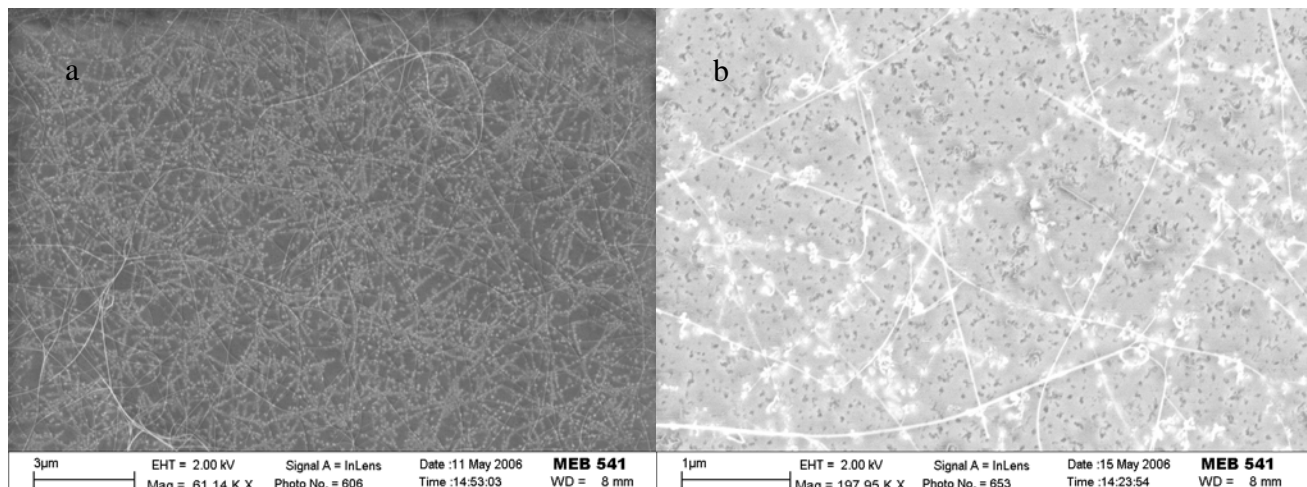


Figure 2: (a) SEM image of the dense Beads on a String pattern grown at 925°C; (b) SEM image of Beads on a String grown at 950°C showing the contrast between bright and dark beads.

The substrate was then placed in a quartz boat, catalyst side up, and inserted into a 1" quartz tube in a 3-zone tube furnace (Lindberg, model number 55367) with a 58434-P temperature controller. After purging atmospheric gases, the substrate was heated for CVD carbon nanotube growth. The new thin film catalyst formulation required that a temperature optimization study be undertaken. Five growth temperatures: 850°C, 875°C, 900°C, 925°C, 950°C were used. After a 5-minute soak in a hydrogen atmosphere, SWCNT growth was achieved by flowing methane, ethylene, hydrogen and humid argon (bubbled through water) over the substrate for 5 minutes. (Flow rates were 1200, 50, 2000 and 730 sccm, respectively). Each growth temperature yielded similar results, indicating the relative insensitivity of growth on temperature. Because growth at 950°C yielded the densest SWCNT network, images and discussion will focus on samples grown at this temperature.

Growth was also repeated on molybdenum grids and 30-100nm thick silicon nitride membranes for transmission electron microscope (TEM) analysis. The grids were attached to the silicon substrate using silver paint. Evaporation of the iron catalyst and CVD were carried out with these substrates as described above.

The vast majority of the described work was undertaken at GSFC. However, growth was repeated at BYU on oxidized silicon substrates. The catalyst on these substrates was evaporated at GSFC, and the growth was carried out as described above using BYU's single-zone CVD growth equipment. At GSFC, the gas flow rates are set using analog rotameters fitted with needle valves; in contrast, BYU's facilities employ digital mass flow controllers to set the flow rates. Both furnaces use a 1-inch outside diameter quartz tube with compression fitting end caps. Similar results to those obtained at GSFC were obtained at BYU, suggesting the process is transferable.

The resulting growth networks on all substrates were then imaged via scanning electron microscopy (SEM), equipped with an in-lens detector, for qualitative comparisons. The in-lens detector is known to cause nanotubes to stand out.¹² At GSFC a LEO Supra 50VP system was used, at BYU we used a FEI XL30 SFEG. Growths on the molybdenum grids and silicon nitride

membranes were also imaged using a transmission electron microscope (TEM) at BYU. Energy-dispersive x-ray spectroscopy (EDX) was used for elemental characterization with both the GSFC SEM and the BYU TEM.

3. RESULTS

A. SEM Analysis

Scanning electron micrographs of the silicon substrates reveal the characteristic BoS pattern, Figure 2a. Figure 2b is a higher magnification image of the BoS pattern. The nanotubes are the thin bright lines which cross the field of view and the beads are the bright features distributed randomly along the lines. Here we discuss the origin and composition of the beads. The contrast setting on the SEM between the Figure 2a and Figure 2b is arbitrary so that the beads are not always as bright as they appear in 1b. However, no matter what the contrast is, it is clear that the beads associated with carbon nanotubes are remarkably bright. Note the dense network of nanotubes with bright beads all along the tube length. The beads near the tubes appear bright indicating that the tubes and bright beads are conducting, whereas those away from the tubes appear dark and are not part of the conducting network.

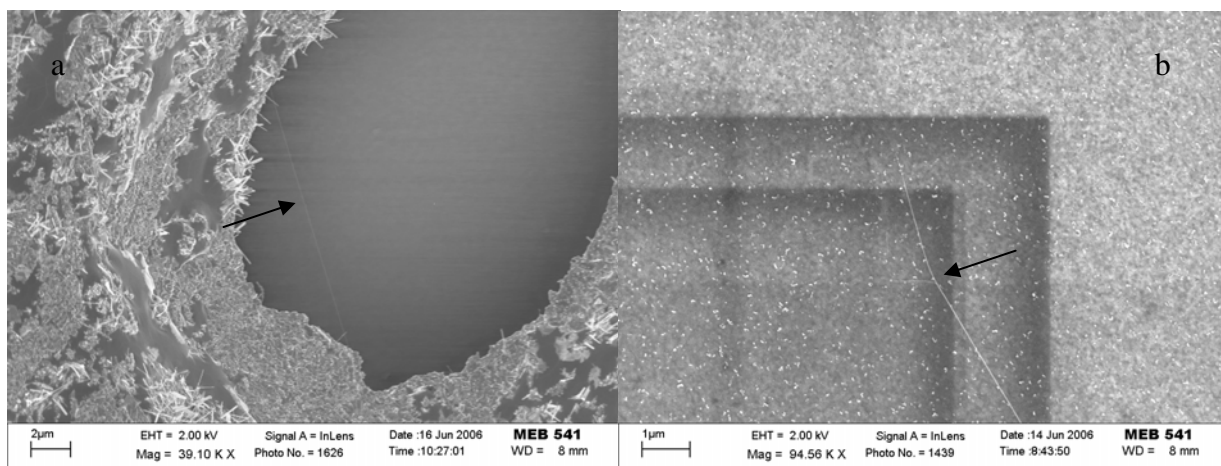


Figure 3: (a) SEM image of SWCNT across molybdenum TEM grid; (b) SEM image of SWCNT across silicon nitride membrane.

Figures 3a and 3b show SEM images of the growth across the molybdenum grid and on the silicon nitride membrane respectively. The bright, thin hair strand-like tubes in both images are characteristic of SEM SWCNT images. The picture frame-like Figure 3b is an artifact of SEM examination of the surface, where the rastering of the beam across the surface creates patterns of carbon deposition that produces a dark color. It should be noted in Figure 3b that the brightness of the beads is not seen to be associated strongly with the progress of the carbon nanotube across the surface. This lack of correlation is likely due to the thickness of the membrane (30nm), relative to the penetration depth of the electron beam, and is consistent with the voltage contrast imaging mechanism described in the literature.¹² EDX analysis of the substrates showed evidence Si, C, O, and Fe, as shown in Figure 4b.. It was not possible to ascertain the composition of the beads and the dark specks exactly due to relatively small ratio of the feature

to beam spot size. The Si and O signals come from the substrate.

B. TEM Analysis

TEM imaging of the BoS pattern was achieved using the growth on the molybdenum TEM grids. Figure 4a shows a TEM image of a bead on a molybdenum grid. Figure 4b shows a TEM EDX elemental analysis of a “bead.” Notice the strong iron peak, as well as the expected peaks for silicon, carbon and oxygen. The TEM's EDX analysis spot on wafers is smaller than the SEM's. Figure 5 shows TEM images of the “strings”. Note the presence of SWCNTs and

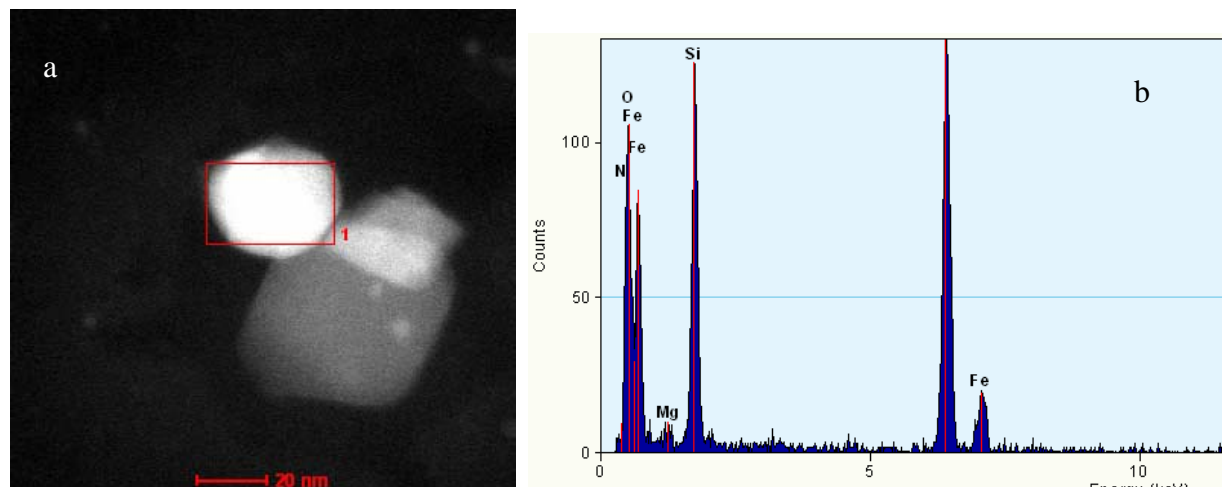


Figure 4: (a) TEM image of a bead from the molybdenum grid sample; (b) TEM EDX analysis of the bead: note the strong iron peaks

carbon nanotube bundles, groups of nanotubes that run together for a distance and then branch off from each other.

5. DISCUSSION

We suggest the following explanation and growth mechanism for the beads on a string pattern. Because of its ability to catalyze SWCNT growth, the indirect evaporation of iron forms a submonolayer of iron on the surface of the substrate with sufficient nanoscale roughness to catalyze SWCNT growth. At growth temperature, this iron beads and collects into particles in order to reduce surface energy. These particles in turn catalyze growth of the SWCNTs which grow vertically from the substrate. Upon removal from the feedstock gasses, the tubes fall to the substrate forming the mat or observed network of nanotubes. This conducting carbon nanotube network and scattered iron particles form the observed beads on a string pattern.

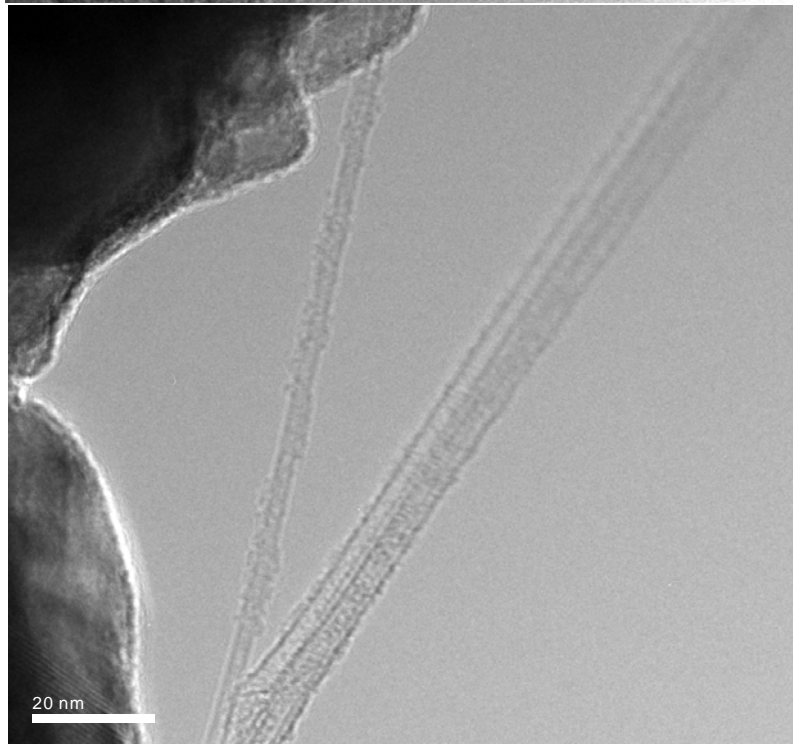
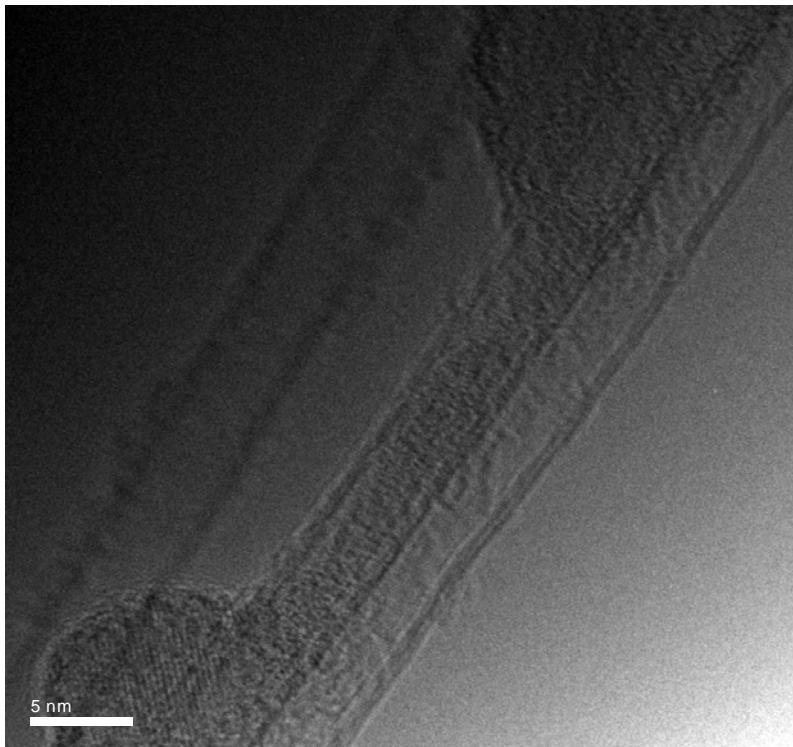


Figure 5: (a) TEM image of SWCNT and double walled carbon nanotubes; (b) TEM image of SWCNT and carbon nanotube bundle. The white bar marks 5 nm in (a) and 20 nm in (b)

6. CONCLUSIONS

The contributions of our group discussed in this paper lie, first, in the areas of depositing the iron catalyst needed for carbon nanotubes growth. Indirectly evaporated iron has been shown to catalyze denser SWCNT growth than achievable with iron nitrate catalyzed growth. An indirect evaporation of iron for use as SWCNT catalyst has been documented. The indirect evaporation technique is a plus for researchers just starting out in thin-film iron-catalyst deposition because the evaporation system is quite a bit simpler than the one used for controlled film deposition below a nanometer thickness.

Second, a previously undocumented SWCNT growth pattern has been identified and characterized. This beads-on-a-string pattern has been determined to consist of iron catalyst particles in a dense SWCNT network.

ACKNOWLEDGEMENTS

The authors would like to thank Dr. Richard Vanfleet and Dr. Jeffery Farrer of Brigham Young University, Provo, UT, for their support in TEM and SEM imaging respectively. We are indebted to Bryan Hicks and members of Prof. Davis' research group who helped us with sample preparation at BYU, including David Hutchinson and Brendon Turner. We are also grateful for the help provided by the management and many members of the GSFC Materials Engineering Branch including Dewey Dove, Bruno Munoz, and Carl Taylor.

Research done at NASA Goddard Space Flight Center by BYU researchers was supported by 2006 GSFC Faculty-Student Team Program (FSTP) (Exploration Systems Mission Directorate) and the Rocky Mountain NASA Space Grant Consortium for Johnathan Goodsell's 2006 support. Additional support at Goddard was through the GSFC Director's Discretionary Fund and Internal Research and Development Funding, Research at BYU was supported but the College of Physical and Mathematical Sciences, the Department of Physics and Astronomy and donations from Marathon Oil Company and V. Dean and Alice Allred to BYU.

REFERENCES

1. H Dai, *Acc. Chem. Res.* **35**, 1035-1044 (2002).
2. T. Tombler, C Zhou, L Alexseyev, J Kong, H Dai, *Nature* **405**, 769 (2000).
3. A. Maiti, A. Svizhenko, and M. P. Anantram, "Electronic Transport through Carbon Nanotubes: Effects of Structural Deformation and Tube Chirality," *Phys. Rev. Lett.* **88**, 126805 (2002).
4. J. Cao, Q. Wang, and H. Dai, "Electromechanical Properties of Metallic, Quasimetallic, and Semiconducting Carbon Nanotubes under Stretching," *Phys. Rev. Lett.* **90**, 157601 (2003).
5. C. Stampfer, A Jungen, C Hierold - Sensors, "Fabrication of Single-Walled Carbon-Nanotube-Based Pressure Sensors," *Nano Letters* **6**, 233 (2006).
6. Y. Su, A. G. R. Evans, and A. Brunnschweiler, "Micromachined silicon cantilever paddles with piezoresistive readout for flow sensing," *J. Micromech. Microeng.* **6**, 69 (1996).
7. P. Dharap, Z Li, S Nagarajiah, EV Barrera, "Nanotube film based on single-wall carbon nanotubes for strain sensing," *Nanotechnology* **15**, 379 (2004).
8. J. H. Hafner, MJ Bronikowski, BR Azamian, P Nikolaev,, "Catalytic growth of single-wall carbon nanotubes from metal particles," *Chem. Phys. Lett.* **296**, 195 (1998).

9. J. Kong, HT Soh, AM Cassell, CF Quate, H Dai, "Synthesis of individual single-walled carbon nanotubes on patterned silicon wafers," *Nature* **395**, 878 (1998).
10. R. G. Lacerda, KBK Teo, AS Teh, MH Yang, SH Dalal, "Thin-film metal catalyst for the production of multi-wall and single-wall carbon nanotubes," *J. Appl. Phys.* **96**, 4456 (2004).
11. K. Hata, DN Futaba, K Mizuno, T Namai, M Yumura, "Water-Assisted Highly Efficient Synthesis of Impurity-Free Single-Walled Carbon Nanotubes," *Science* **306**, 1362 (2004).
12. T. Brintlinger, Y.-F. Chen, T. Durkop, E. Cobas, M. S. Fuhrer, J. D. Barry, and J. Melngailis, "Rapid Imaging of Nanotubes on Insulating Substrates," *Appl. Phys. Lett.* **81**, 2454 (2002).

Figure Captions

1. Iron catalyst was deposited using an indirect evaporation method, in which the substrate faces away from and out of the line-of-sight of the source (not to scale).
2. (a) SEM image of the dense Beads on a String pattern grown at 925C; (b) SEM image of Beads on a String grown at 950C showing the contrast between bright and dark beads.
3. (a) SEM image of SWCNT across molybdenum TEM grid; (b) SEM image of SWCNT across silicon nitride membrane
4. (a) TEM image of a bead from the molybdenum grid sample; (b) TEM EDX analysis of the bead: note the strong iron peaks
5. (a) TEM image of SWCNT and double-walled carbon nanotubes; (b) TEM image of SWCNT and carbon nanotube bundle. The white bar marks 5 nm in (a) and 20 nm in (b)

